DESIGN AND TESTING OF A MODEL WING SECTION FOR A HUMAN POWERED AIRCRAFT

P. Mardanpour*,, W.R. Krüger*, H. Haddadpour**, D. Hoffmann***

*** DLR - Deutsches Zentrum für Luft- und Raumfahrt**
Institut für Aeroelastik, Göttingen, Germany
**** Sharif University of Technology,**
Aerospace Engineering, Tehran, Iran

Keywords: *aeroelasticity, human powered aircraft, light-weight wing, LCO*

Abstract

Human powered aircraft (HPA) have a number of special design features. They are of a high aspect ratio, have a very low weight and are consequently equipped with very flexible wings. The aeroelastic behaviour of such aircraft is of great interest.

At the Institute of Aeroelasticity of the German Aerospace Center (DLR), a 1:3 scale section of a light-weight wing has been built and tested in an open wind tunnel with comparable Reynolds number of model and original HPA. Representative values for geometry and stiffness were derived from an original HPA design.

During the experiment, vibration tests of the structure were performed. During the wind tunnel test, static and transient investigations were performed. Finally, using a modified mass distribution, the flutter point was determined numerically and experimentally, and a limit cycle oscillations (LCO) could be observed in the experiment. Measurements indicate that the LCO is due to massive flow separation at positive and negative high angles of attack.

1 Introduction

1.1 Human Powered Aircraft -

A Human Powered Aircraft (HPA), as its name indicates, flies with the power that a human supplies. Power is transmitted to the plane's propeller by pedals and the propeller provides the thrust. HPAs are characterized by their long wingspan providing a large surface and their considerable light weight, due to the relatively low speed and the restrictions of the pilot's power. Because of this, manufacturing such a plane needs a technology with great precision in design, creative mind and organized teamwork. Minimizing the weight of different parts and energy dissipation in the system and increasing the planes overall efficiency are the key goals in the design process.

Human Powered Aircraft wings are as a rule very flexible, light and with large deflection during flight condition. Flexible high-aspect-ratio wings have the potential to undergo large deflections, which under certain flight conditions can reach the geometric nonlinear range of the wing structure; thence the aeroelastic analysis will need special consideration.

1.2 "Fly the Sky by Myself" - a Brief Historical Overview of Human Flight

Man has always dreamt of flight, and human-powered flight has been one of his most premier thoughts. One of the oldest narratives of flight is that of Keikavoos Shah, king of ancient Iran, who about 4000 years ago managed to fly by tying the strong birds he had grown to his throne. The idea of human-powered flight was first approached by tying wings, which led to no success in experiment. In Greek mythology, Daedalus and Icarus built wings of bird feathers, strings and wax to escape their prison in Crete. According to other historical documents, the first human being who flew successfully was an Iranian scientist who tied wings to himself and escaped from Second Shahpoor's prison about

1800 years ago. After that about 1400 years ago an Iranian Muslim scientist, called Farnaas, flew successfully by tying wings to himself.

As technology progressed, man's ancient dream came true, by the construction of "Human-Powered Aircraft". In 1959, Henry Kremer offered a prize for a maneuverable HPA to cover a defined course and distance. The prize invoked a great deal of enthusiasm, leading to the construction of 30 aircraft in 17 years, including aircraft from Great Britain, Japan, the United States and France. Finally, the first Kremer Prize was won in late 1977 by an HPA called Gossamer Condor, piloted by Bryan Allen and designed by Paul B. MacCready. The same team also won the second Kremer Prize two years later with the Gossamer Albatross [1]. Since then, about 100 more HPA were built in Germany, Japan, Greece, New Zealand, South Africa, Canada, Singapore, U.S., England, etc. In most of these countries, the projects were supported and sponsored by many companies and organizations. For instance, the Daedalus project was supported by more than 50 companies and organizations, direct cost of which was $1.2 million and 170000 man-hours of actual work was devoted to it [2].

1.3 Aeroelasticity

Aeroelasticity is the study of the effect of aerodynamic forces on elastic bodies. Aeroelasticity includes certain phenomenon involving mutual interaction among inertial, aerodynamic and elastic forces. Based up on the interaction between these three forces the aeroelastic problems can be classified as static aeroelastic problems (divergence, control system reversal, load distribution) and dynamic aeroelastic problems (flutter, buffet, dynamic response). [3] gives the following definitions of those phenomena:

• Divergence: A static instability of a lifting surface of an aircraft in flight, at a speed called the divergence speed, where the elasticity of the lifting surface plays an essential role in the instability.

• Control system reversal: A condition occurring in flight, at a speed called the control reversal speed, at which the intended effects of displacing a given component of the control system are completely nullified by elastic deformations of the structure.

• Flutter: A dynamic instability occurring in an aircraft in flight, at a speed called flutter speed, where the elasticity of the structure plays an essential part in the instability.

• Buffeting: Random vibration of aircraft structural components due to unsteady aerodynamic forces usually associated with separated flow. Wake behind wings, nacelles, fuselage pods, or other components of the airplane may generate excitation of downstream components.

• Dynamic response: Transient vibration of aircraft structural components produced by rapidly applied loads due to gusts, landing, gun reaction, abrupt control motions, moving shock waves, or other dynamic loads.

• Load distribution: Influence of elastic deformations of the structure on the distribution of aerodynamic pressures over the structure.

1.4 Case Study

In this study a high aspect ratio wing based on a design for an HPA was considered. It is based on the design of FARNAS, a joint project between Sharif University of Technology and Amirkabir University of Technology for "designing and building an ultra-light airplane powered by human", named after the historic scientist mentioned above. Figure 1 gives the general layout of the aircraft.

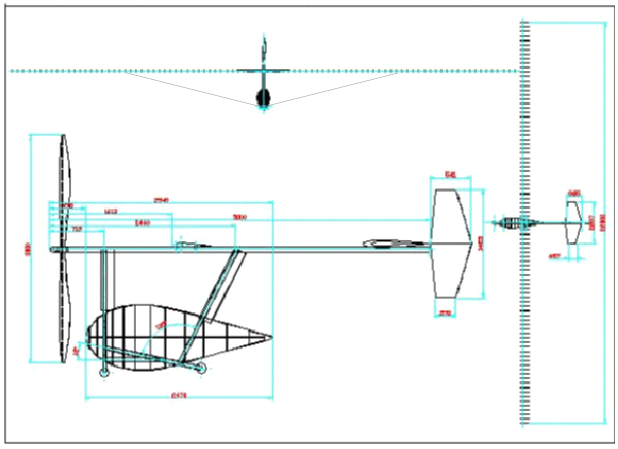

Fig. 1. FARNAS HPA general layout

The aircraft is equipped with a wing with a span of 22 m and an aspect ratio of 44. At a semi-span of 5.5 m, a kevlar chord controls the upward bending of the wing, see Figure 2. Center of gravity, and elastic axis of the wing are located at 25% cord length. The wing spar is a circular epoxy carbon structure with a constant cross-section up to the middle of the wing; from the location of the kevlar cord, the spar tapers conically into a smaller diameter at the wing tip. The ribs are out of fibre glass epoxy carbon, the skin of the wing is out of mayler.

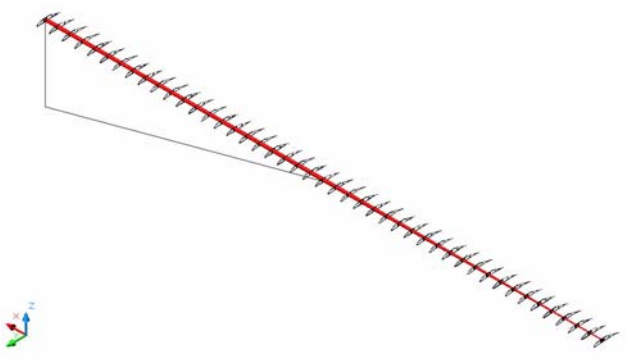

Fig. 2. FARNAS HPA wing design

The aircraft was designed to fly at an altitude of 20 m with a cruise velocity of 12 m/s. This speed corresponds to a Reynolds number of approximately 500000.

The wing profile is a Worthman FX-76-MP140 which has been chosen for its high lift at low velocities. Figure 3 gives the 2D polar of the selected wing profile.

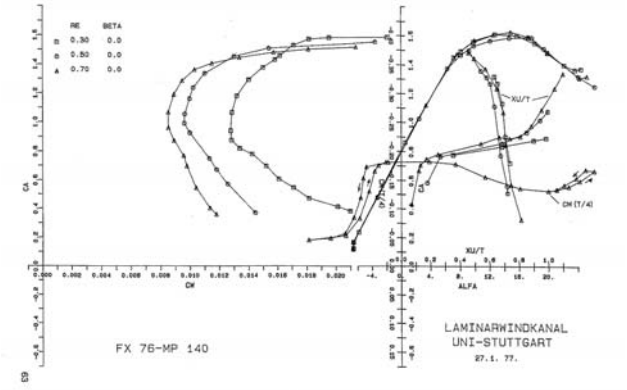

Fig. 3. Polar for FX-76MP140

Given the low speed of operation, a strong dependency of the aerodynamic properties on the Reynolds number can be seen. Worth noting is also a steep gradient of the aerodynamic moment between -10º and 0º of angle of attack which is a potential aerodynamic source of the amplitude-limited aeroelastic instability seen in the experiment which was eventually performed on a scaled wing.

1.5 Objectives of this study

The original objective of the study is to determine the aeroelastic response of a human powered aircraft wing experimentally. Wing flexibility coupled with the long span leads to the possibility of large deflections and nonlinear structural behavior during normal flight operation. Unsteady linear aerodynamics theory and nonlinear structure yield a nonlinear aeroelastic model. However, the large scale of HPA made tests on a full model impossible during the project described.

In the present work, wind tunnel tests are performed on a scaled wing. The primary objective of this study is thus to observe experimentally the dominant properties of an aeroelastic high aspect ratio wing. Even though it is evident that a direct extrapolation of test results to the real aircraft will not be possible, the experiment is useful to understand the basic physical correlations and to evaluate the design methods and codes to make a reliable prediction of static and dynamic aeroelastic phenomena of human powered aircraft.

2 Wind Tunnel Model Design

2.1 Scaling Considerations

In this section, the basic considerations for the model design will be discussed. Considering the fact that the aeroelastic model must be dynamically scaled as well as having the proper external geometric shape, flutter model similarity and dimensional analysis of the wing have been investigated. The geometric scale is usually fixed by consideration of wind tunnel size and other applicable limitations such as the maximum model span that the tunnel can accommo-

date which should not exceed 0.8 of the tunnel width.

In order to scale the wing for wind tunnel tests, similarity laws and scaling theory should be considered. The first consideration has to be the purpose of the model investigation, i.e. is the focus on static or dynamic problems, and the important forces, i.e. the magnitude and relation of inertial, elastic, aerodynamic and gravitational forces.

In order to have exactly the same load distribution as well as elastic deformation shape as the full scale it is necessary to build a model which has the characteristics as below:

- The same aerodynamic shape,
- The same elastic stiffness distribution in both torsion and bending span wise and chord wise,
- The same ratio of inertial forces to aerodynamic forces,
- The same mass distribution,
- The same ratio of bending and torsion stiffness,
- The same location of elastic axis and center of gravity.

Usually, not all of those requirements can be met at the same time. On a model with scaling factor M, to meet the condition of flutter similarity would require a wing density of 1/M. Considering that already the original human powered aircraft is extremely light, it is virtually impossible to build a scaled model with the required density.

It was finally decided to drop the requirement of strict dynamic scaling and to build a model wing with the following assumptions:

- Comparable Reynolds number to the HPA wing,
- Similar static deflection of model wing to HPA wing.

The decision was driven by the available low speed wind tunnel with a test section of 1m×0.8m, running up to 60 m/s. Reynolds number might be the best characteristic number which accommodates the wing aerodynamic properties.

The minimum chord length is defined by manufacturing possibilities and instrumentation. The original aerodynamic profile should be kept. Taking all constraints into consideration, a scaling factor of M=3.33 was chosen. The resulting chord length was 14.5 cm. Keeping the Reynolds number constant required a wind speed of 40 m/s. Since the test section size is only 1 meter in width and, to avoid wing tip effects we could only use 75% to 80% of the wind tunnel section, it was decided to design a model with a span of 70 cm, representing the deflection of the outer 1/4 span of the original wing. The effect of the inner 3/4 of the wing on the total deflection was represented by an elastic wind tunnel attachment. Two configurations were tested, the plain wing and the wing with an added mass of 146 g, mounted at the wing tip 14.5 cm behind the elastic axis.

2.2 Wing Design

Following the considerations laid out above, a model with the following characteristic was designed and built in the DLR Institute of Aeroelasticity in Göttingen, see Figure 4.

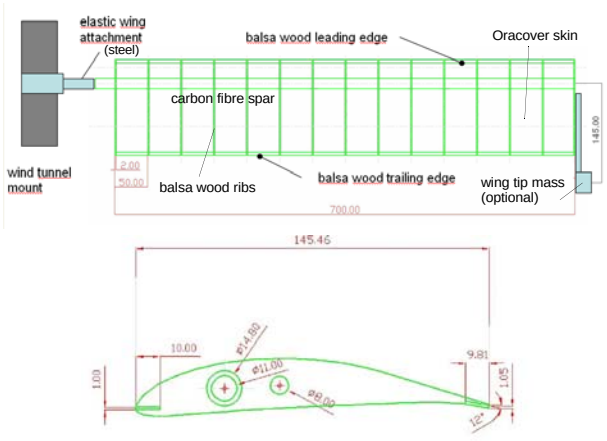

Fig. 4. Model wing, top view and rib

The wing consists of a tube spar of constant thickness, 12 averagely spaced ribs and a foil skin. The spar is a carbon fibre tube with an outer diameter of 14.8 mm and an inner diameter of 11 mm, with a measured average bending stiffness of EI = 117 Nm^2 and a torsional stiffness of GJ = 22.4 Nm^2. The total weight of the spar is 1400 g.

The ribs are manufactured out of balsa wood, the rib shape, determining the profile of

the wing, was cut on a plotter saw. For main spar and wires two holes were designed. The relative distance of the ribs is smaller than for the original HPA for better airfoil accuracy. For the leading edge and the trailing edge, thin rectangular strips of balsa wood were cut and placed perpendicular to the ribs during wing span. These spars are designed to maintain the geometrical form of the profile along the span. Their elasticity in bending is EI = 0.1 Nm^2 and thus very small compared to the carbon fibre spar.

For the skin, the lightest material available was Oracover foil [7]. As mentioned above, small rib spacing and leading and trailing edges were use to support the foil since it contracts when it is heated to form the wing surface. One open question is that the exact influence of the skin, as a component, on elasticity has not been determined.

For a second configuration, amounting for an added mass of 146 g, 14.5 cm behind the elastic axis, was installed at the wing tip.

2.3 Attachment

The attachment was made out of regular ST37 steel and was not objected to the air flow. Its bending and torsional stiffness was derived from the scaled stiffness of the actual wing. The right hand side circular section of the attachment was fed into the spar tube and was fixed by means of glue, the left hand side was mounted in the wind tunnel support. The elastic section of the attachment was 50 mm long, 12 mm wide and 4 mm thick.

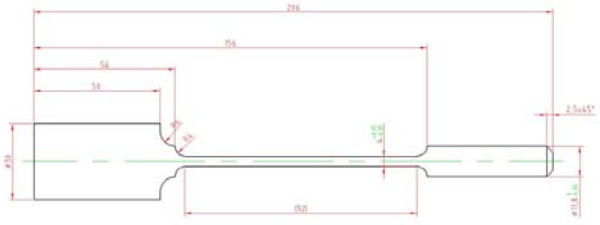

Fig. 5. Flexible steel attachment of wing

2.4 Instrumentation and Data Acquisition System

Data acquisition was performed using accelerometers and photo-optical measurements. An additional set of strain gauges, originally designed to measure attachment loads, were applied but could not be used during the experiment due to amplifier failure.

The wing was equipped with seven accelerometers by PCB Piezotronics [8]] glued to the ribs in the locations shown in Figure 6. The weight of the accelerometers was 3 g each. As not to distort the original model properties, a low sensor weight is, of course, essential for use with a light-weight model.

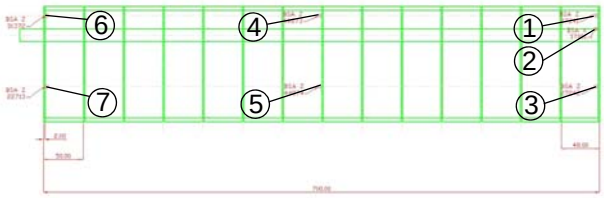

Fig. 6. Location of accelerometers

In parallel to the acceleration data, a signal generator was included which could provide a step triangular function with a step at each 0.1 s as a reference for synchronization.

For the static tests, pictures by a digital camera with a resolution of 4 Mio pixels were taken and analyzed by performing pixel counts against a reference scale. The method worked surprisingly well, the reading error being in the order of 0.5 mm.

In order to acquire the data, 8 channels of a 16 channel USB-based data acquisition box from Measurement Computing Cooperation Company [9] were used. 7 channels were used for accelerometers, and one for synchronization.

Data was acquired using the software SoftWIRE [9], a library-based block-oriented modelling approach by Measurement Computing Cooperation Company. Depending on the test, data was scanned with a sampling rate of 200 Hz to 1000 Hz and written to a text file. For post processing of the acquired data, MATLAB [10] and SCILAB [11] were used.

3 Structural Properties of the Model

3.1 Static Deflection Tests

For the static deflection test of the wing, the wing was mounted as a cantilever beam and was loaded with a concentrated force at the wing tip. The tip displacement was measured by a length scale with respect to a reference point on the trailing edge of the wing. For the torsional stiffness, a defined torque was introduced in the wing tip. The total wing deflection at the tip was determined to be 0.0062 m/N, the total lag deflection was 0.003 m/N.

3.2 Ground Vibration Tests (GVT)

A Ground Vibration Test (GVT) is commonly performed to validate the natural frequencies and mode shapes of an elastic system. The basic concept is to excite the structure and measure the response at certain locations through the vehicle. The response is then analyzed to estimate the natural frequencies and mode shape of the linear model. The primary use of this information is to check the estimated mass and stiffness properties used in flutter and dynamic load calculations by comparing the experimental frequencies and mode shapes with the ones that are calculated. The experimental data serve as the basis for new calculations. Two basic different methods of excitation are possible, the phase resonance and the phase separation method.

3.2.1 Methods

In the phase separation method, the excitation of the structure is a pulse generated by hammer in a single point of the structure. Optimally, the pulse will excite all of the normal modes of the structure. The response of the structure can then be expressed as a linear combination of sinusoidal oscillations of these normal modes with the respective natural frequencies.

Using Fourier transformation (FFT) of the time domain response, it is possible to extract the distribution of amplitudes of the modes (or mode shapes) in the frequency domain. The frequencies of the peaks of the estimated frequency response functions can be identified as the natural frequencies of the structure. The advantage of this method is the short time to perform the test. If the amplitude of the excitation impulse is known, structural damping and generalized masses of the structure can be calculated from the decay of the response.

In the phase resonance method sinusoidal forces of various frequencies and amplitudes are applied at several points of the structure such that one desired mode after another is correlating with the excitation and responding predominantly. The motion of different points are in phase or counter-phase. The excitation has 90 degrees phase with respect to deflection/acceleration. To cover a certain frequency range, sweeps of the excitation frequency have to be performed, changing frequencies either stepwise or in a continuous fashion. Generalized masses and structural damping are obtained from the known magnitude of the excitation input. Generalized masses can be obtained by adding small masses to the structure and measuring the change in the natural frequency. From the difference between the original and the new frequency and the change in mass, the original mass can be deducted.

Comparing the methods, phase separation gives faster results since only a few excitations are necessary and the analysis is quick, however, for complex structures with a large number of modes in a small frequency range, the identification of a mode and distinction between modes can be difficult. For complex structures, it is usually advantageous to use sinusoidal excitation rather than the pulse type because sinusoidal excitation permits a concentration of available power on one mode after another so that the desired answers can be obtained.

The disadvantage of phase resonance is that scanning time through all the modes is much higher in comparison with the pulse type excitation. Therefore, vibration tests can be started with pulse type excitation to identify critical regions which are then scanned by phase resonance approaches.

3.2.2 Results

Before the wind tunnel test, only measurements using the phase separation approach were performed, on the original wing and on the wing with the added wing tip mass. Only later was a phase resonance test performed, the results being in very good correlation with the original results.

The structure (wing) was mounted to the wind tunnel mount and excited in different points at the wing tip by a hammer. The time domain response was recorded by the accelerometers and the data processed through an FFT analyzer to determine the natural frequencies.

To obtain the mode shape for a frequency corresponding to the natural frequency of the system, the amplitude of the sensors was plotted versus the sensor positions. This plot gives the mode shape corresponding to the peak frequency identified as the natural frequency.

When sensor 1 and 3 are in phase, bending is observed, sensor 1 and 3 with opposite deflection indicates a wing torsion mode. Table 1 gives the results for the vibration tests up to 100 Hz.

mode	frequency [Hz] (wing without mass)	frequency [Hz] (wing with tip mass)
bending (plunge)	8.5	4.0
lag (fore/aft)	20.0	9.0
torsion (pitch)	85.5	22.8
2nd bending	-	78.0

Table 1: Wing modes and natural frequencies

As an example, the frequency response for sensor number one for the wing with added tip mass is plotted in Figure 7. The resonance frequencies for bending and torsion are clearly visible in the plot. As sensor one was placed in z-direction, the lag mode does not appear in the plot.

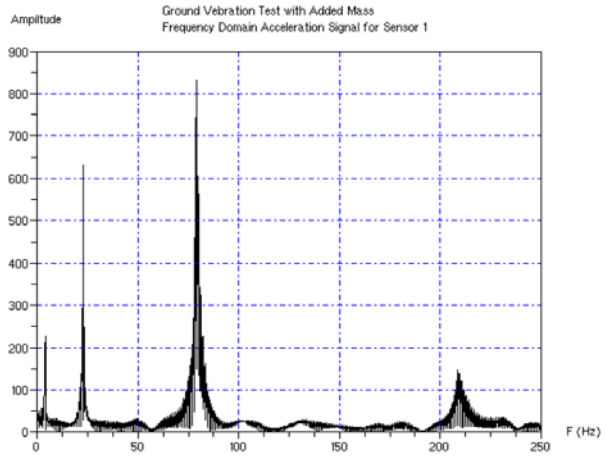

Fig. 7. Vibration test results (wing with added mass, sensor 1)

3.3 Flutter calculation

To have an estimation of the critical flutter speed for the wind tunnel test, a new calculation with updated data from GVT and static deflection test was performed. The new calculations were performed by ZAERO software, with a linear structural and a linear aerodynamic solver. Figure 8 gives the results of the flutter calculation. The flutter speed was determined to be 37.0 m/s.

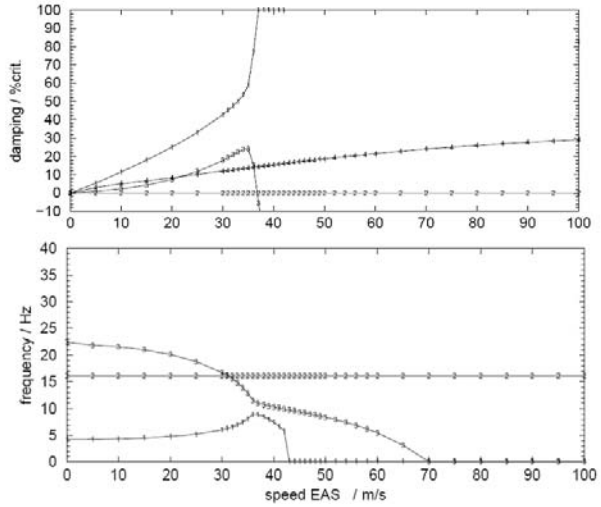

Fig. 8. Results of flutter calculation

4 Wind Tunnel Tests

4.1 Wind Tunnel Test Setup

The aeroelastic wing model was tested in the subsonic wind tunnel of DLR in Göttingen, with one meter rectangular open test section. The tunnel has a maximum operating speed of 60 m/s which is well beyond the designed flutter boundary of the model with the added tip mass.

The wing is mounted horizontally in the tunnel and is the only component exposed to the flow. The wind tunnel mount was assumed to be rigid and could be set manually to different angles of attack in free stream direction. Motion in vertical bending and torsion direction is considered, the maximum deflection allowed is 0.2 m at the wing tip. The experiment consisted of static and dynamic test. Figure 9 shows the installation of the wing in the wind tunnel.

Fig. 9. Set-up of wind tunnel experiment

4.2 Static Wind Tunnel Test

In this test program, the wing tip displacement was measured in different velocities and different angles of attack. The displacement was measured by evaluating pictures taken during the test at given velocities. The wind tunnel speed was varied in a range from 0 to 35 m/s for angles of attack from -10° to 10° in steps of 5°. However, due to the model design, eventually not all combinations of wind speed and angles of attack could be reached. Due to the elasticity of the wing attachment, aerodynamic wing loading was restricted up to 50 N.

The results of the statically deflected wing show a strong dependency of aerodynamic properties on flow speed in the low velocity region. Clearly the influence of low speed aerodynamics can be seen. For low wind speeds, large separation both at the upper and lower side of the wing is responsible for the non-linear lift development over angle of attack. Only for speeds higher than 15 m/s does the flow attach and the lift slope comes closer to a linear behaviour. It is important to note for the discussion of the limit cycle found in the flutter test that measurements below -5° were difficult at wind speeds greater than 15 m/s because the wing vibrated strongly due to separation.

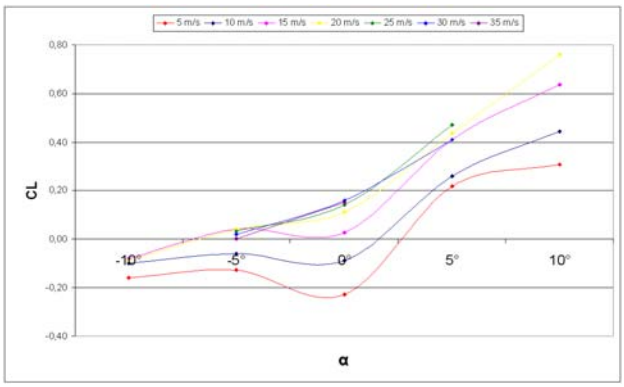

Fig. 10. Result of static wind tunnel test: lift polar

4.3 Transient Motion Experiment

In a first experiment, a transient motion of the wing without added tip mass was measured. For that purpose, the wing was deflected by a force of 5 N downwards (i.e. against the lift) by means of a string tied to the wing tip. The string was cut, and the response of the wing recorded. Figure 11 shows an overlay of the time plots of the motion of the wing for different wind speeds,

- black: 0 m/s,
- blue: 10 m/s, and
- green: 20 m/s

The effect of aerodynamic damping can clearly be seen. For the given speed range, damping increases notably for higher wind speeds. Closer analysis of the results is an open topic.

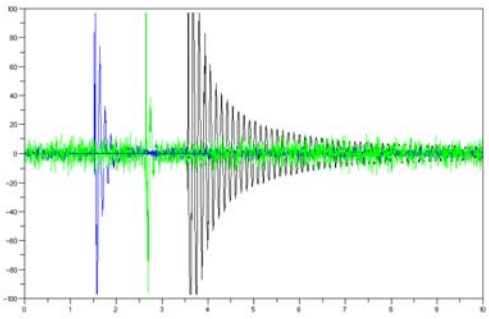

Fig. 11. Time plots of transient motion

4.4 Flutter Test

In this test the goal was to capture dynamic instability, i.e. flutter or limit cycle oscillation, in wing behaviour. This test was performed for the wing with added mass at the tip. For the experiment, the wing was fixed at a suitable angle of attack and the velocity was increased up to the linear flutter speed. The flutter point could successfully be reached for a static angle of attack of -5°.

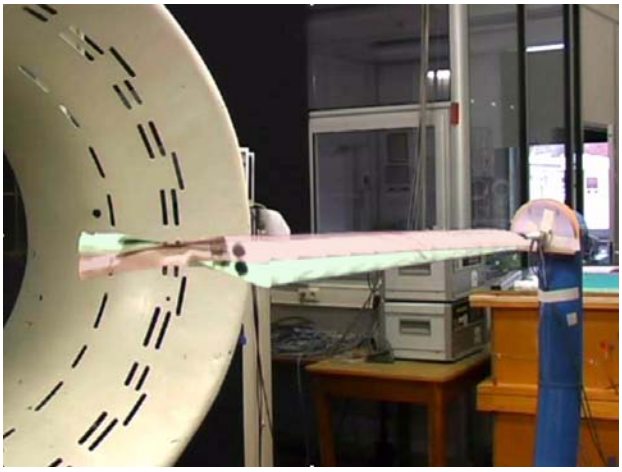

Fig. 12. Limit Cycle Oscillations of wind tunnel model

The instability set in at 34.7 m/s very rapidly and settled into an LCO which was clearly visible, see Figure 12, and remained constant until it was suppressed either by lowering the wind speed or by manually stopping the oscillations. During the LCO, the angle of attack varied between -12.5° and +2.5°.

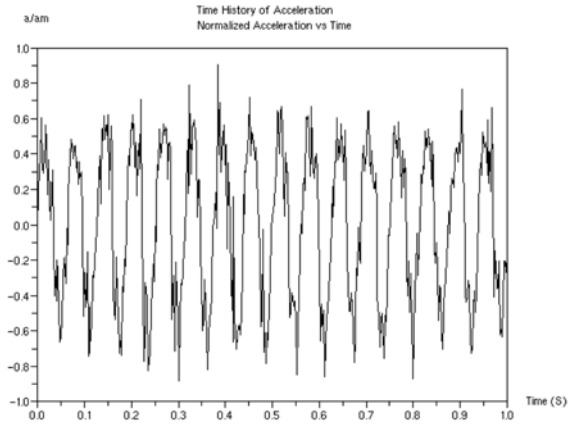

Fig. 13. Accelerations during LCO at sensor 1

As the instability occurred, the acceleration was recorded in the time domain. The measurement was obtained by comparing accelerations at sensor 1, see Figure 13, and at sensor 3. Velocity and position were obtained by integrating the acceleration data. Looking at the position data, an additional low frequency motion could be observed. Thus, to plot velocity against position, a second order high-pass filter with a cut-off frequency of about 1 Hz was applied to the data. Ideally, plotting velocity against position should give an ellipse for harmonic motion. Tilting of the ellipse is due to the high-pass filter which shifts the phase of the position signal by a small negative amount, see Figure 13.

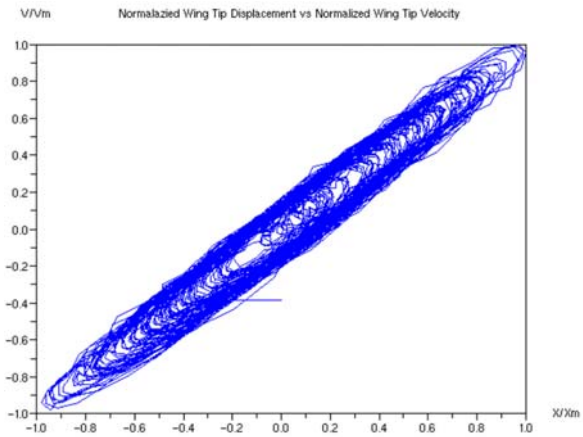

Fig. 14. Velocity against position for LCO

The frequency response was obtained by applying FFT to the time domain data. Clearly the frequency of the LCO of 16.5 Hz is visible.

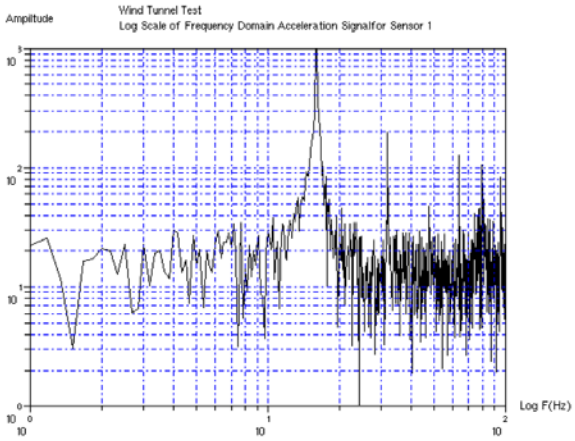

Fig. 15. Frequency response of the LCO

Due to the boundary conditions of the model design and the wind tunnel, a parametric study of the influence of variations of angle of attack and the resulting high deflections could not be performed since the wing left the central flow field even for small positive angles of attack at the necessary wind speeds. Therefore, the work had to be focused on the analysis of the limit cycle oscillation found at -5°.

5 Discussion

The model wing was built based on a design for a human powered aircraft, keeping similar profile and Reynolds number, but changing the elastic properties such that the test set-up consisted of a rather rigid wing on an elastic attachment. Most of the elasticity, both in vertical bending and in pitch was concentrated in that attachment. Static results were obtained by digital photographs, calibrated by wind-off force measurements, dynamic results were obtained by acceleration measurements.

The results of the static tests clearly indicate the strong dependence of the properties of the profile on Reynolds number. The experiment operated in a region where small changes in Reynolds number results in large changes of lift and moment. The phenomenon is well known, literature gives indications that the main reasons are large changes, even jumps, in the transition point from laminar to turbulent flow and flow separation [4], [5]. As the wind speed increases, the flow attaches to the airfoil and the lift curve is more linear. In any case, strong separation occurs for large positive and negative angles of attack which were reached during the dynamic experiment.

The transient motion experiment showed nicely the dependence of aerodynamic damping on flow speed. However, a thorough evaluation of the experiment has yet to be done.

The flutter experiment was performed with the wing with an added tip mass as the original wing had no tendency to flutter due to its layout with elastic axis, center of mass and aerodynamic center all being on, or very close to, the 25% chord. Thus, the added mass de-tuned the wing so that the flutter point lay in the region which could be reached in the wind tunnel.

The flutter speed has been calculated by linear theory and was very well predicted. At the flutter point, the motion settled into a limit cycle oscillation (LCO). Even though no unsteady aerodynamic data is available, even the steady aerodynamic data which was measured justifies the conclusion that the dominant factor of the LCO is of aerodynamic source. From the measurements we saw that the angle of attack during the LCO fluctuates between -12.5° to 2.5°, compare also Figure 12. This is a range in which the aerodynamic moment of the airfoil sections varies very much in the polar diagram. Additionally, we saw during the steady measurements that at -10° separation was very strong. It is therefore safe to assume that this separation is the main factor limiting the energy brought into the system and thus limiting the oscillation at the otherwise unstable point.

Looking at the velocity and position data, a low frequency motion could be observed which cannot totally be accounted for at present. However, Harash et. al. [6] report a similar behaviour, and internal discussions indicate that a feed-back through the wind tunnel flow might be a cause for such effects.

6 Conclusions and Future Work

With a model wing in two variants, static and dynamic experiments were performed in a wind tunnel. The static experiments showed well the properties of the wing at low Reynolds numbers. With a modified wing, an LCO could be observed and evaluated in the operational range of the available wind tunnel.

Some points are suggested for further investigation:

Numerical investigations of the observed effects should continue. Numerical simulation of transient motion and LCO will aid in the understanding of the phenomena and increase validation of the available design methods.

A study of effects of structural or geometrical non-linearity of a high aspect-ratio wing would be possible and attractive with a similar set-up. However, the current wing structure was far too stiff and the attachment spring too soft to study those topics. In a future wing, the attachment should being stiffer and a closer correlation of bending and pitch frequencies should be designed in the model. To be mode independent from a specific profile, a symmetric profile should be used. With that approach it should be possible to investigate e.g. the influence of variations of angle of attack on the flutter point or the LCO.

Summarizing it can be stated that the Farnas HPA wing layout is well suited to study static problems, but not dynamic problems. This could be done by using a modified wing. Feedback to the full-scale aircraft is limited, however, code validation and transfer of design expertise is possible. Technical advice can be deducted from the experiment.

Acknowledgements

P. Mardanpour performed his Master's Thesis with a range of numerical and experimental tasks during the experiment described in this paper. Prof. H. Haddadpour was his supervisor at Sharif University of Technology. The authors would like to thank their colleagues from the DLR Institute of Aeroelasticity, especially Dr. Fritz Kießling for his continuous technical and scientific support and Prof. Hönlinger, as well as the team from the 1m wind tunnel of the DLR Institute of Aerodynamics and Flow Technology.

7 References

[1] http://ourworld.compuserve.com/homepages/j_d_mcintyre/hpag.htm: The Royal Aeronautical Society Human Powered Flight Group, London, GB, 1994.

[2] Dorsey, G.: The Fullness of Wings: The Making Of A New Daedalus. Penguin, USA,1992.

[3] Bisplinghoff, R. L., Ashley, H. & Halfman, R. L., Aeroelasticity, Cambridge, Mass: Addison-Wesley Publishing, 1995.

[4] Mueller, T.J.: Aerodynamic Measurements at Low Reynolds Numbers for Fixed Wing Micro-Air Vehicles. In: RTO Educational Notes: EN 9, Development and Operation of UAVs for Military and Civil Applications. NATO/RTO 2000.

[5] Low Reynolds Number Aerodynamics on Aircraft Including Applications in Emerging UAV Technology. RTO-EN-AVT-104. NATO/RTO 2003, publ. 2005.

[6] Harash, E., Abramovich, H., Weller, T.: Further Technion Studies on Aeroelastic Experiments of Composite High-Aspect-Ratio Wing Model. TAE - 962, IDM and Technion, Research & Development Foundation Ltd., Haifa, Israel, 2005.

8 References for Software and Hardware

[7] http://www.oracover.de/xml/

[8] http://www.pcb.com

[9] http://www.measurementcomputing.com

[10] http://www.mathworks.com

[11] http://scilab.org